J. Geomag. Geoelectr., **49**, 523–542, 1997

Variation of Rock Magnetic Parameters and Paleointensities over a Single Holocene Lava Flow

H. BÖHNEL[1], J. MORALES[1], C. CABALLERO[1], L. ALVA[1], G. MCINTOSH[1], S. GONZALEZ[2], and G. J. SHERWOOD[2]

[1]*Instituto de Geofísica, UNAM, Mexico City 04510, Mexico*
[2]*School of Biological and Earth Sciences, Liverpool John Moores University, Byrom Street, Liverpool, L3 3AF, U.K.*

(Received February 15, 1996; Revised June 30, 1996; Accepted October 10, 1996)

A recent (2000 BP) lava flow from central Mexico has been sampled along a vertical profile with 55 cores covering a total flow thickness of 6.6 m. A wide range of physical and magnetic parameters have been studied to characterise the samples: Curie temperature and saturation magnetisation as intrinsic properties; density, magnetic susceptibility and remanence intensity as bulk properties; Königsberger Q-factor and hysteresis parameters as coercivity parameters. All parameters vary smoothly over the profile, most probably due to grain size variation of the magnetic minerals present in the samples. Optical observations indicate that the main opaque minerals are deuterically oxidised titanomagnetites (C3–C5) and ilmenites (R2–R3), which increase in size away from the edges of the flow. Paleointensity (PI) was determined using the double heating Thellier-Thellier method with pTRM checks. According to reliability parameters (f-, g-, and q-factor) the obtained PIs are of reasonable to good quality. PI shows marked variation with vertical position in the flow, across a range of about 25 to 125 μT, with most samples having a PI between 50 and 100 μT. The flow-mean PI of 72 μT is higher than the present day field, consistent with global data for this time-period. No obvious correlation could be found between PI and any other measured parameter. The variation of PI with vertical position in the flow may show some systematic behaviour. It is important, therefore, to sample a flow both horizontally and vertically in order to obtain a reliable paleointensity.

1. Introduction

Lavas are generally considered to be the best recorders of geomagnetic behaviour, paleomagnetically speaking. Yet individual flows may show considerable variability in their magnetic properties (Watkins and Haggerty, 1965; Ade-Hall *et al.*, 1968a; Wilson *et al.*, 1968; Lawley and Ade-Hall, 1971; Peterson, 1976; Herzog *et al.*, 1988; Audunsson *et al.*, 1992), and the extent to which this impacts on the paleomagnetic signal recorded in the flow will limit its potential resolution. Natural remanent magnetisation (NRM) intensity and stability have been shown to be far from uniform, NRM intensity in particular varying by more than a factor of 10 within individual flows. In most cases this variation seems related to high temperature (HT) deuteric oxidation of the remanence-bearing titanomagnetites, the development of which can be highly variable within any single flow giving rise to complex intra-flow NRM distributions (e.g. Wilson *et al.*, 1968; Peterson, 1976; Herzog *et al.*, 1988).

NRM directions may also exhibit some variability. Samples with low NRM stability often show greater scatter about the flow-mean direction (e.g. Watkins and Haggerty, 1965; Wilson *et al.*, 1968; Herzog *et al.*, 1988). This is associated with the development of a magnetically soft secondary overprint and on alternating field demagnetization to relatively low fields (<40 mT) the directions converge with the flow-mean value. Herzog *et al.* (1988) describe a flow showing large directional changes towards its base. The amplitude of these changes varied laterally and they were ascribed to (variable) viscous movement below the Curie temperatures of the constituent magnetic grains. Coe *et al.* (1995) found dramatic and repeatable changes in intra-flow directions. These showed no obvious correlation with rock magnetic parameters,

leading the authors to suggest a geomagnetic origin for the variation.

Few studies have investigated the variation of paleointensity (PI) determinations within individual flows. Smith (1967a, b) and Ade-Hall *et al.* (1968b) measured multiple samples from a single flow, although the samples were selected on the basis of their oxidation state and as such do not define a systematic study throughout the complete flow. Nonetheless the studies showed that PI determinations and their reliability varied quite considerably. Rolph (1992) noted that in some cases samples taken from Mount Etna flows yielded anomalously high PIs, and detailed investigation of two recent Etna flows indicated intra-flow PI variation of up to 60% (Rolph, submitted), apparently related to changes in grain size/oxidation state of the remanence carriers.

Furthermore, PI experiments conducted on samples obtained from different exposures of the same lava flow in Mexico City yielded significantly different results (see next section). It was this observation that prompted the present study, the main objective of which is to see how PI determinations vary with vertical position in the flow.

The question of intra-flow PI variation is of importance in evaluating the reliability of data included in the paleointensity database (Tanaka *et al.*, 1995) for general access and evaluation. Sampling for PI experiments has often not been done in a systematic manner covering all parts of a flow, but was rather adjusted to the outcrop conditions. In former times it was also common to take just 1 to 3 samples, and it is not clear if the results from these samples are representative of the flow-mean PI. The use of such data to analyse the long-term behaviour of the geomagnetic field could therefore be misleading.

2. The Xitle Lava Flow

The flow selected for the present study is located in the southern part of the Basin of Mexico (Fig. 1), extending northwards some 10 km from the cinder cone of Xitle volcano. It covers an area of about 80 km^2 and large parts of southern Mexico City are built on the flow surface, including the campus of the National University. The lava is composed of olivine basalt and is of considerable archeological interest because of its effect on the environment of the early urban centre of Cuicuilco. Numerous ^{14}C analyses have been carried out since Libby (1955) to fix this impact in time (see review in Cordova *et al.*, 1994): apparent ages cluster around 2400 BP and 2000 BP. These ages in part were obtained from samples taken from baked sediments at different depths below the lava flow and this may go some way in explaining the range of age determinations. Recently, Delgado (personal communication) have obtained two ^{14}C dates of 1945 ± 55 BP and 2025 ± 55 BP for the flow. This data has good stratigraphic control and suggests that the data cluster at around 2000 BP best represents the age of the flow.

The northern end of the lava flowed over alluvial and reworked volcanic sediments of the Basin of Mexico. At several places, including the sampling site, this interface is exposed and the burned sediments may be observed for more than a metre depth. As these sediments are of low remanence intensity, we exclude any local effects which could have deflected the thermoremanent magnetisation (TRM) from the geomagnetic field direction or influenced the TRM intensity of the flow significantly.

Previous studies of the Xitle lava flow reveal strongly varying PIs: Nagata *et al.* (1965) report a PI of 57.2 ± 5.4 μT for samples close to the Cuicuilco pyramid; Gonzalez-Huesca (1992) reports values between 54 μT and 120 μT for site S9 (Fig. 1), with a site-mean PI of 67 ± 10 μT; Morales-Contreras (1995) obtained from outcrop JM mean values of 59 ± 11 μT and 49 ± 5 μT, depending on the method applied for the PI determination. Common to all studies is the finding that PI is higher than the present field intensity of 43 μT. This is in broad agreement with archeomagnetic results from southern USA (Sternberg, 1989) and other data from the rest of the world (McElhinny and Senanayake, 1982), which show PIs some 30–40% higher than the present day at around 2000 BP.

An outcrop was selected where the lava is exposed from top to bottom, and where sampling was possible along a vertical profile. In this outcrop no horizontal interfaces are visible and the rock is clearly composed of a single flow. The lowermost part (cores 50–55) of the sampled profile is reddish and porous, resembling a scoriae in texture and colour. Above that part and up to about 4 m (cores 21–49), the lava

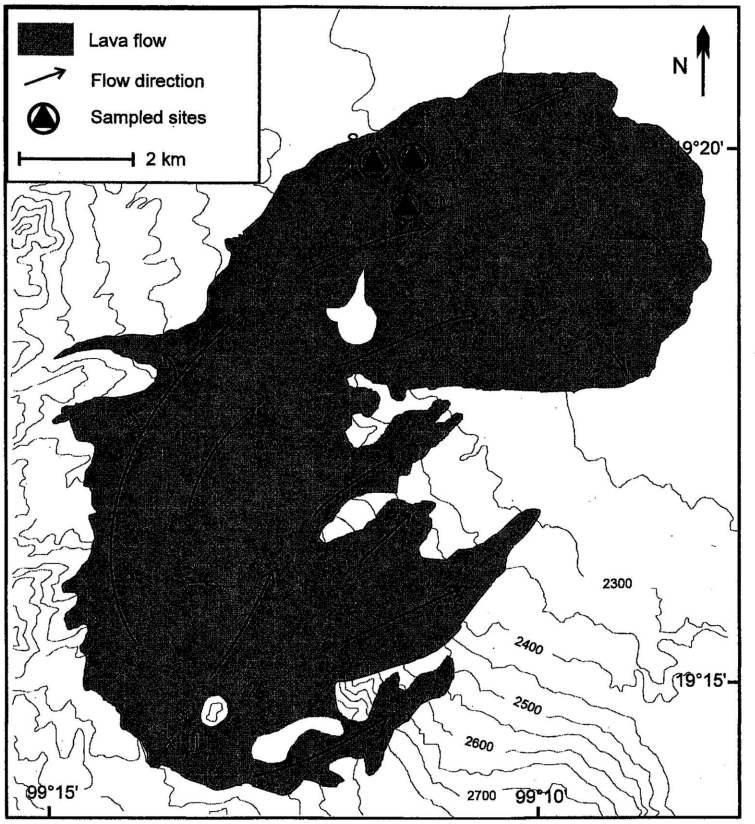

Fig. 1. The Xitle lava flow. CU-8 marks the outcrop of the present study, S-9 and JM sites of former studies. Modified after Cordova *et al.* (1994).

is very homogeneous and almost without vesicles. Moving upwards (cores 1–20) the number of vesicles increases rapidly. They are oriented horizontally and include large pipe vesicles which reach up to about 15 cm across. It was difficult to obtain unbroken cores from this part of the flow because of the abundant vesicles. In the massive lower part this was easier, although many cores broke prior to orientation due to the glassy, brittle nature of the basalt.

3. Sampling and Laboratory Procedures

The flow had a thickness of 6.59 m at the sampling site. Sampling was conducted by means of a scaffold, providing easy access and allowing cores to be taken along a straight vertical line. Cores were recovered using a gasoline drill with a diamond bit and oriented in situ with a magnetic compass. 55 cores were obtained, distributed evenly over the flow, of which only 15 were oriented in situ. The other 40 cores broke during drilling for reasons explained above. The cores were cut into 2–5 samples, one of which was used for rock magnetic studies in the Geomagnetism Laboratory in Liverpool; the remainder were employed for rock magnetic and PI experiments conducted in Mexico. Additional core-chips were used for some rock magnetic experiments.

The volume of the samples was determined from their height and diameter. All samples were weighed with a laboratory balance, for normalisation of bulk magnetic parameters commonly based on standard samples (magnetic susceptibility and remanence intensity). A density value was calculated from these

parameters, which reflects the space occupied by vesicles in each sample.

Magnetic susceptibility was measured with a Bartington bridge at low and high frequency of the measurement field. During the PI experiments, the change of magnetic susceptibility of the samples was monitored using a Molspin Minisep bridge.

Magnetic hysteresis loops were determined with a Princeton Measurements Corporation alternating gradient magnetometer (model MicroMag 2900) in fields up to 1 T. This instrument was also used to obtain acquisition curves of isothermal remanent magnetisation (IRM) and backfield IRM from the same sample piece. In these experiments a small piece (20–50 mg) from one of the samples or from a core-chip was used. From the MicroMag hysteresis experiments the following parameters were derived: magnetic coercive force H_c, saturation magnetization M_s, remanent saturation M_{rs}, all in a maximum field of 1 T. All samples exhibited saturation in a 1 T field, although they showed a varying paramagnetic contribution. This contribution was subtracted from the hysteresis loop, assuming that the increase of magnetisation above 0.8 T was entirely due to the paramagnetic effect. All hysteresis parameters were derived from this corrected curve. From the backfield IRM experiments the remanence coercivity force H_{cr} was determined.

Variation of magnetic susceptibility was measured between –196°C and 5°C, using a sample piece or core-chip. This was enveloped together with a thermocouple in plasticene and immersed in liquid nitrogen until reaching a temperature equilibrium. Then it was introduced into the low-temperature sensor of a Bartington bridge and the susceptibility measured during warm up.

Thermomagnetic curves were determined using a horizontal magnetic balance in the Liverpool laboratory. For this purpose a piece of the sample used previously for low-temperature susceptibility measurements was crushed. The powder was introduced into the balance and heated up to 700°C in air. The variation of the induced magnetisation in a constant field of 0.35 T was recorded during heating and subsequent cooling to 100°C. Curie temperatures, T_c, were determined graphically using the tangent method (Grommé *et al.*, 1969). Selected parallel sample pieces were also studied in the paleomagnetic laboratory at Fort Hoofddijk (Utrecht), using the magnetic balance described by Mullender *et al.* (1993). These measurements gave very similar results except that the observed T_cs were on average 25°C lower than those obtained with the Liverpool balance. We assume that this difference is due to a temperature hysteresis and/or offset in the Liverpool system, as here T_cs were always around 600°C, too high for the kind of magnetic minerals (Ti-poor titanomagnetites, see below) observed in the flow. Therefore a correction of –25°C was applied to the T_c values determined from the thermomagnetic curves measured in Liverpool.

4. Paleointensity Experiments

The PI was determined using the Thellier method as modified by Coe (1967). Samples were first heated and cooled in the absence of a laboratory field (thermal demagnetisation), using a Magnetic Measurements thermal demagnetiser (MMTD1). This was then repeated in the presence of a 50 μT laboratory field to produce a partial thermoremanent magnetisation (pTRM). At selected temperatures a pTRM check was inserted after thermal demagnetisation: the pTRM acquisition was repeated for a previous (i.e. lower) temperature step to check for physico-chemical alteration at the temperatures reached so far which would have produced changes in the pTRM capacity. In some cases multiple pTRM checks were used. The heating time was 10 minutes, and the samples were held at the selected temperature for a further 20 minutes. Cooling was performed as fast as possible, needing between about 30 and 60 minutes. After each temperature step the magnetic susceptibility was measured to trace major changes of the bulk magnetic properties. Results are presented in Arai diagrams, where the loss of NRM is plotted versus the acquisition of pTRM. The PI is obtained by multiplication of the gradient of the best-fit line to the points in the Arai diagram with the value of the laboratory field. To obtain the best-fit line and its error we used the algorithm proposed by York (1966).

From the data used to construct the Arai plots several parameters were derived which give quantitative information about the quality of the obtained PI (Coe *et al.*, 1978): the gap factor (g) describes

how the data points are distributed along the best-fit line. If the points are evenly distributed $g = 1$; if the points are concentrated at the extremes of the line $g = 0$. The fraction factor (f) is a measure of the remanence fraction used to determine the best-fit line and has a value of 0(1) if none(all) of the remanence is used. Both factors are used together with the gradient of the best-fit line and its error to calculate a quality factor (q) where $q > 0$ and may have values of several tens for very good PI results.

5. Magnetic Mineralogy

In order to determine the magnetic mineralogy we have made both direct observations of the magnetic minerals and measurements of a range of magnetic properties.

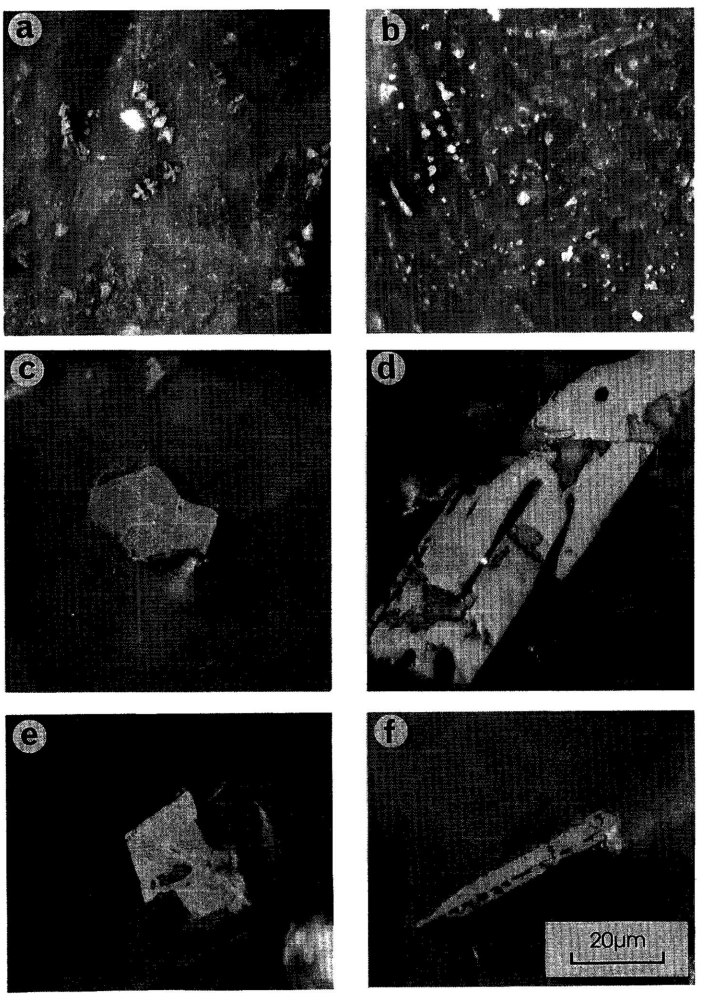

Fig. 2. Photomicrographs using the reflected light microscope, showing examples of magnetic minerals at different heights within the flow. All photos are taken using a 125× oil immersion objective and are at the same scale. a) Top of flow (sample 1) - skeletal titanomagnetite, C1–C3 and ilmenite R1. b) Base of flow (sample 50) - dissemination of very small subhedral titanomagnetite and ilmenite. c) Central part of the flow (sample 35) - titanomagnetite C4 with trellis structure. d) Central part of the flow (sample 35) - ilmenite R2–R3. e) Lower central part of the flow (sample 41) - titanomagnetite C5 with trellis structure. f) Lower central part of the flow (sample 41) - partially skeletal ilmenite R2.

5.1 Ore microscopy

We made polished sections from the majority of the samples along the profile. A reflected light microscope with oil immersion objectives of 10×, 40× and 125× was used to identify the magnetic minerals. The classification used for the description of the magnetic minerals follows Haggerty (1976), using C1–C7 for the deuteric oxidation class of titanomagnetite (TM) and R1–R7 for ilmenite.

According to the observations made with the ore microscope it is possible to divide the lava flow into three zones:

a) The uppermost part of the flow (samples 1 to 3) shows small euhedral titanomagnetites and ilmenites with skeletal textures (Fig. 2(a)). In this part of the flow the magnetic minerals have an oxidation state of C2–C3 and R1 respectively; the size of the minerals is approximately 2–5 μm.

b) The central part of the flow (samples 4 to 48) contains larger euhedral to subhedral crystals of titanomagnetites and ilmenites with trellis and sandwich structures. The oxidation states are higher with typical values of C3–C5 and R2–R5. The size of the titanomagnetites is between 20–30 μm and the ilmenites are up to 150 μm in length (Figs. 2(c)–(f)). In general, the minerals are larger towards the centre of the flow.

c) The lowermost part of the lava flow (samples 49 to 55) shows small euhedral titanomagnetites and ilmenites, in disseminated form or with skeletal textures (Fig. 2(b)). The state of oxidation is probably C2, in the case of the skeletal grains, but some grains with C3–C5 are also present. The grain sizes vary from about 1–5 μm. Some samples have some hematite pigment, though this is unlikely to contribute significantly to the remanence.

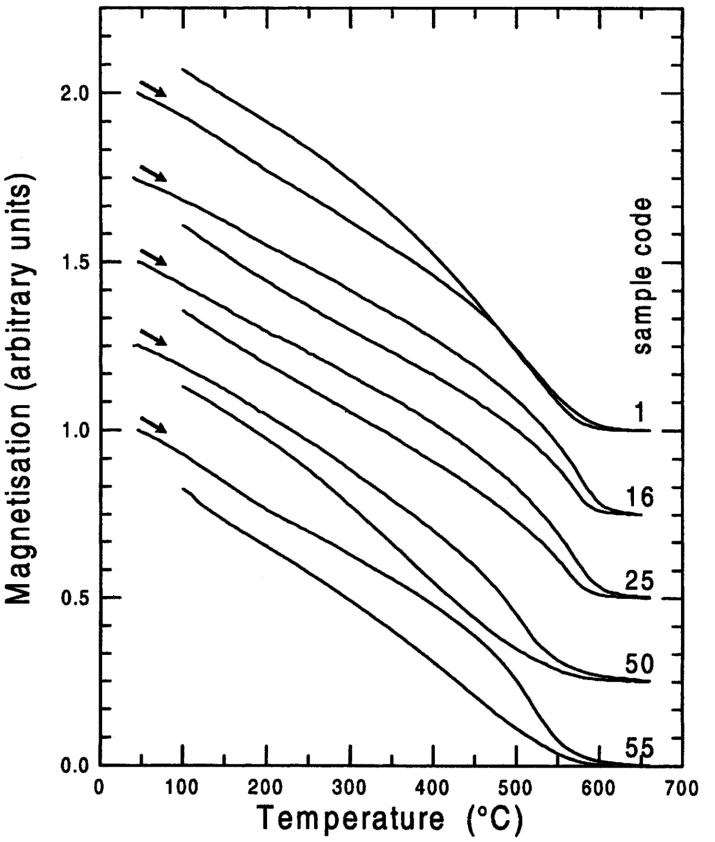

Fig. 3. Strong-field induced magnetisation versus temperature for representative samples from different heights above flow base.

One important characteristic of the Xitle lava flow is the large quantity of ilmenite present, which in the uppermost and lowermost parts of the flow is in needle form with oxidation states of R1–R2. The intermediate part of the flow, however, has large ilmenite grains (often >100 μm) with oxidation states of R3–R5.

5.2 Magnetic properties

Two intrinsic parameters have been studied: T_c and M_s. These properties depend only on the chemical composition and crystal structure. Figure 3 shows the different types of thermomagnetic curves observed over the profile. The vast majority of the samples exhibit thermomagnetic curves similar to those of samples 16 and 25, with T_c around 575°C to 580°C (corrected value). The magnetic minerals responsible are interpreted to be titanium-poor TM (magnetite). In all but one sample the cooling curves have a lower

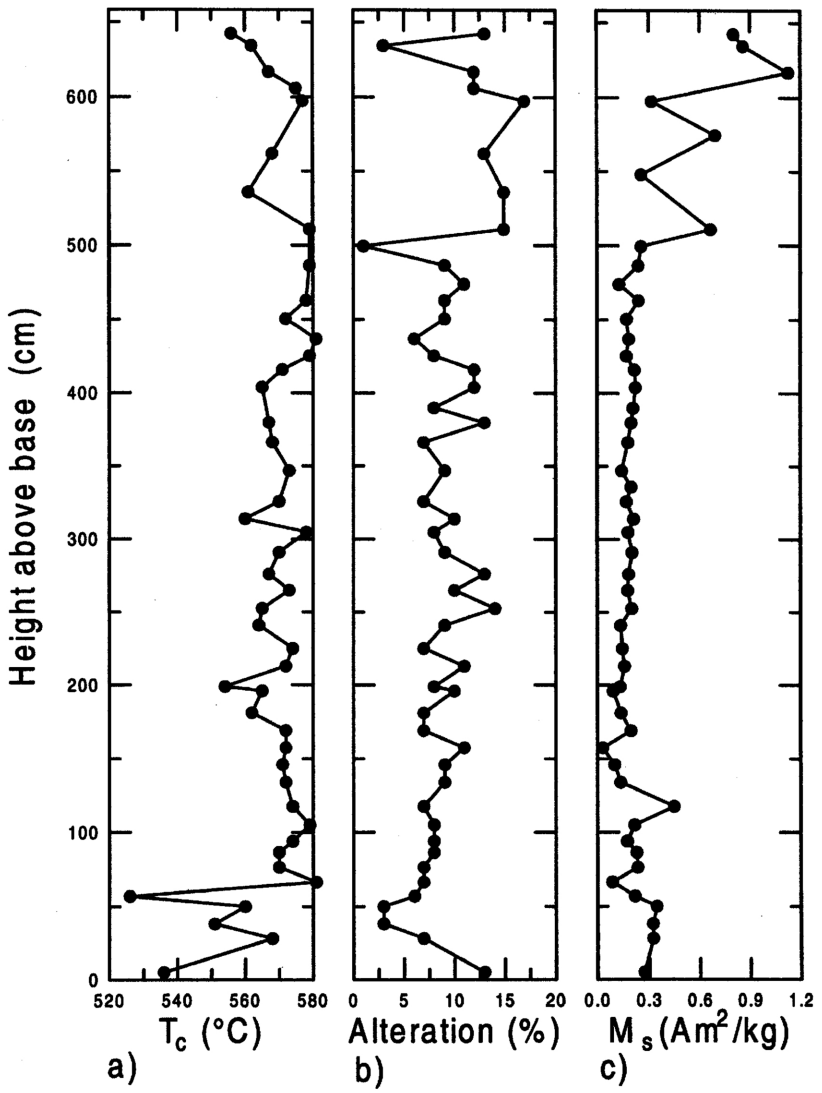

Fig. 4. Variation with height above flow base of (a) Curie temperature, T_c, (b) alteration (% difference between the heating and cooling legs of the thermomagnetic curve at 100°C) and (c) saturation magnetisation, M_s.

magnetisation than the heating curve, possibly indicating some oxidation of the TM. Sometimes a slight inflection of the thermomagnetic curve was recognisable at temperatures around 200°C, implying the presence of a small quantity of titanium-rich TM minerals. Only very near to the base of the flow did these minerals appear in larger quantity, as visible in the well expressed inflection of the curve of sample 55. The uppermost sample, sample 1, exhibits different behaviour, the cooling curve passing above the heating curve. This sample may have a small amount of low temperature oxidation producing cation-deficient magnetite which decomposed upon heating. From the thermomagnetic experiments we conclude that the dominant magnetic minerals in the Xitle flow are titanium-poor TM (magnetite).

T_c is plotted in Fig. 4(a) versus the height above the base of the flow. Small variations of T_c with height with amplitudes of about 10°C may be explained by a varying oxidation degree of the TM. This very small

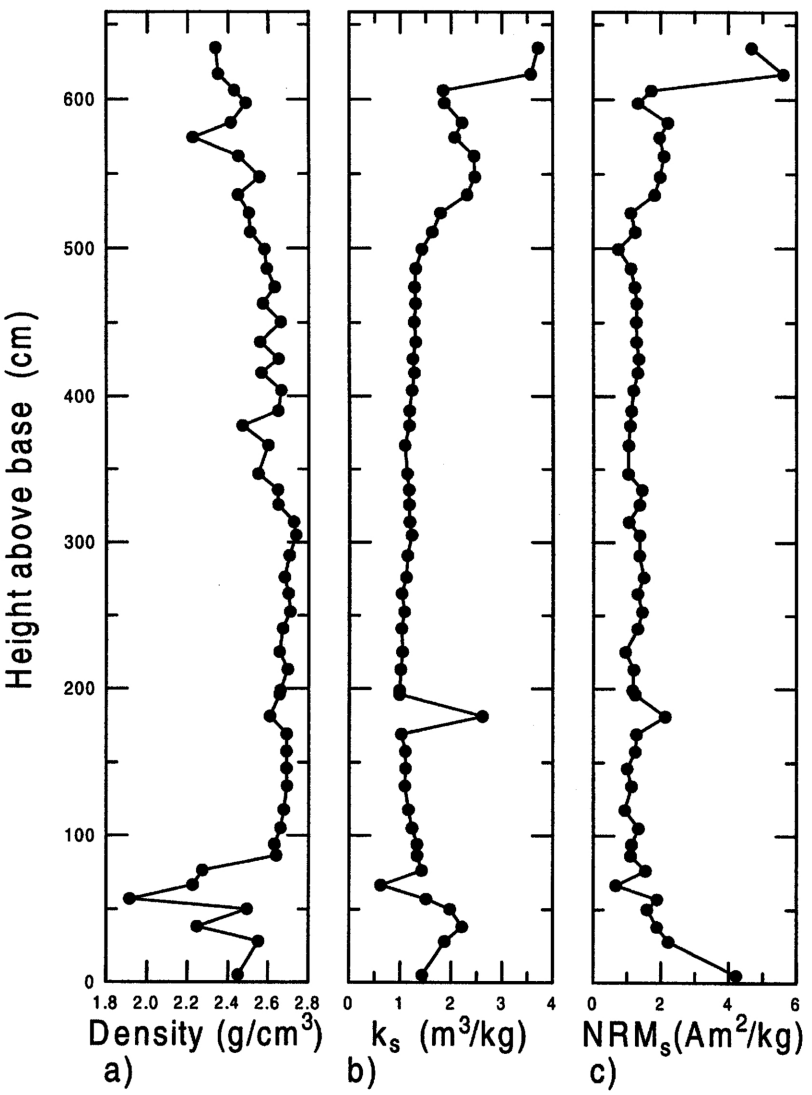

Fig. 5. Variation with height above flow base of bulk parameters (a) density, (b) mass specific magnetic susceptibility, k_s, and (c) mass specific NRMs intensity.

variation is similar to that observed by Wilson *et al.* (1968) in a 16.8 m thick flow with a slightly higher variation of oxidation degree.

We can attempt to characterise the reversibility of the thermomagnetic curves in order to gain an indirect measurement of the degree of alteration suffered during heating. For this we look at the difference between the heating and cooling curves at 100°C, calculated as a percentage. This value increases with increasing alteration (decreasing reversibility) irrespective of whether there is an increase in magnetisation on cooling (such as for sample 1) or a decrease (all other samples). The results are plotted in Fig. 4(b). Throughout most of the flow the alteration lies between 5–12%, with a slight increase up to 15–16% between 510–600 cm above the base. Such low values highlight the overall reversibility of the curves and are encouraging in that they suggest thermal alteration might not be a major problem during the PI experiments. M_s, normalised by weight, is plotted versus height in Fig. 4(c), showing that M_s is highest at the top of the flow with a slight rise also at the base. The higher M_s values may be explained by a higher concentration of magnetic minerals, as T_c did not indicate any important compositional change. Other parameters influenced by the concentration of magnetic minerals (magnetic susceptibility, NRM intensity) also show such a variation with height (see below). Wilson *et al.* (1968) also observed an increase in M_s towards the top of a 16.8 m thick flow, correlating that with a decrease in HT-oxidation degree. The oxidation degree seems to vary in the Xitle flow as well, as our optical observations indicate, though it is difficult to correlate the increase in M_s with a change in oxidation state. Assuming that minerals with 80 Am^2/kg (typical value for low-titanium TM, e.g. Hunt *et al.*, 1995) are responsible for the magnetic properties, the volume content of these minerals in the lava was estimated: over most of the profile this would give only 0.25 vol.%, which is rather low for a volcanic rock.

A number of physical and bulk magnetic properties are available for the samples, shown in Fig. 5 versus height. Density is fairly uniform over most of the flow, except near to the lower and upper surfaces (Fig. 5(a)). Here the large quantity of vesicles reduces the density, and the irregular variations from sample to sample depend on the volume occupied accidentally by such vesicles.

The magnetic susceptibility (Fig. 5(b)) was normalised by the sample weight to take into account the space occupied by vesicles. Over most of the profile susceptibility shows little variation, with small irregularities around 70 cm and 180 cm. Minimum values are observed at approximately 200 cm, and from there increase towards the upper and lower limits of the flow. Above 600 cm susceptibility varies strongly (even between samples from the same core). Similar variations, observed in previous studies, have been attributed to grain size variations of the magnetic minerals (e.g. Petersen, 1976; Herzog *et al.*, 1988). The grain size may depend on the cooling rate of the flow and also on the HT oxidation state of the magnetic minerals which reduces the magnetically effective grain size with increasing oxidation (e.g. Wilson *et al.*, 1968). Like M_s, susceptibility shows a peak above 500 cm and this is true for the NRM intensity, also normalised by the sample weight (Fig. 4(c)). Therefore in this part of the profile the volume content of magnetic minerals increases.

TRM and magnetic susceptibility generally show inverse variation with grain size (e.g. Hunt *et al.*, 1995). In the present case the susceptibility variation may be explained as an increasing content of single domain (SD) particles. The microscopically observed TM grains, although generally large, have undergone high-temperature oxidation, thus reducing their effective grain size. We therefore reach the conclusion that most of the TM grains behave as SD grains, where magnetic susceptibility approaches minimum values. Near the extremes of the flow, where rapid cooling could have preserved smaller TM grains, a larger quantity of SD grains of sizes near the SD-multidomain boundary may be present. Such grains have much higher susceptibility values (Hunt *et al.*, 1995) and could, at least partly, explain the susceptibility increase in those parts of the profile.

Variation of magnetic susceptibility at low temperatures depends on the composition and grain size of the magnetic minerals present in the sample (Senanayake and McElhinny, 1981; Radhakrishnamurty, 1985). Figure 6 shows typical examples of susceptibility, normalised by the value at 5°C, versus temperature. For most samples (e.g. samples 14–49, Fig. 6) susceptibility decays strongly while warming to 5°C, and in some cases the relative susceptibility ratio ($RS = K_{-196°C}/K_{5°C}$) reaches values of 2.6. Gonzalez-

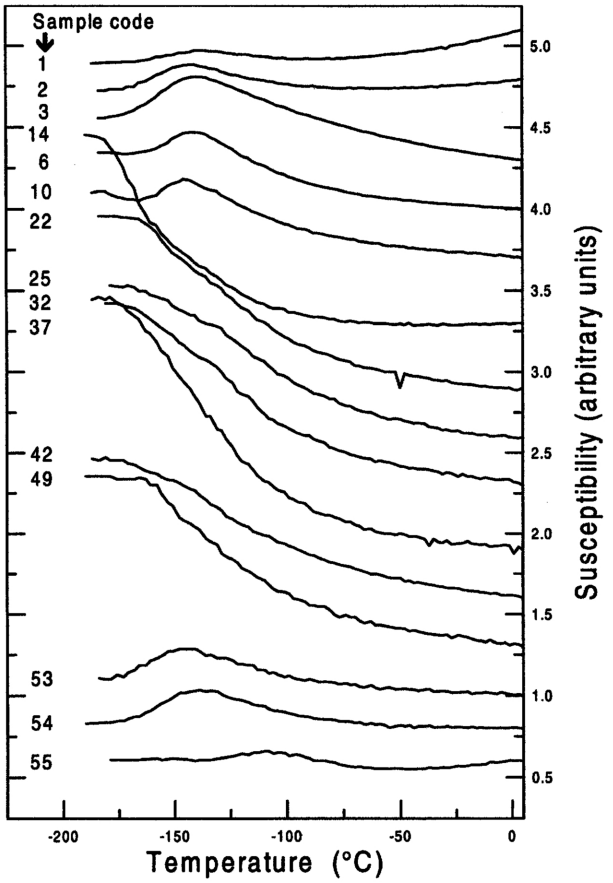

Fig. 6. Low-temperature variation of normalised magnetic susceptibility for representative samples at different heights above flow base.

Huesca (1992) noted similar behaviour for this flow. We propose that the variation is due to the presence of ilmenite which over this temperature range is paramagnetic. The largest *RS* values are observed in the centre of the flow, which is where the largest ilmenite grains are observed. Samples near the flow margins exhibit susceptibility variations as for samples 2 and 54 (Fig. 6). Such curves, with the characteristic peak around –150°C, are indicative of the presence of multidomain (MD) magnetite (e.g. Radhakrishnamurty, 1985). However, other rock magnetic parameters (see above and below) appear to indicate an increasing contribution of SD particles towards the flow margins. We believe that the majority of the grains at the flow edges are single domain, but a few are large enough to produce the MD susceptibility peak.

The remaining parameters refer to the coercivity and thus to the granulometry of the TM minerals. The Königsberger Q-factor, defined as the ratio of remanent to induced magnetisation, is considered as a stability parameter depending mainly on the grain size of the magnetic particles in a sample. Q varies between 20 and 30 in most parts of the flow, tending to lower values above 300 cm and showing a minimum at about 500 cm (Fig. 7(a)). Towards the flow extremes, Q increases rapidly. According to this parameter, the smallest particles in the Xitle flow are found below 300 cm and near the flow margins.

Coercive force H_c displays minor variations along the profile (Fig. 7(b)). Only the lowermost sample shows a very different coercive force, probably due to low grain size of the TM. This magnetic parameter seems to be characterised by the properties of the bulk TM grains present in each sample, dominating the properties of less abundant grains with higher coercivity, as described by Day *et al.* (1977).

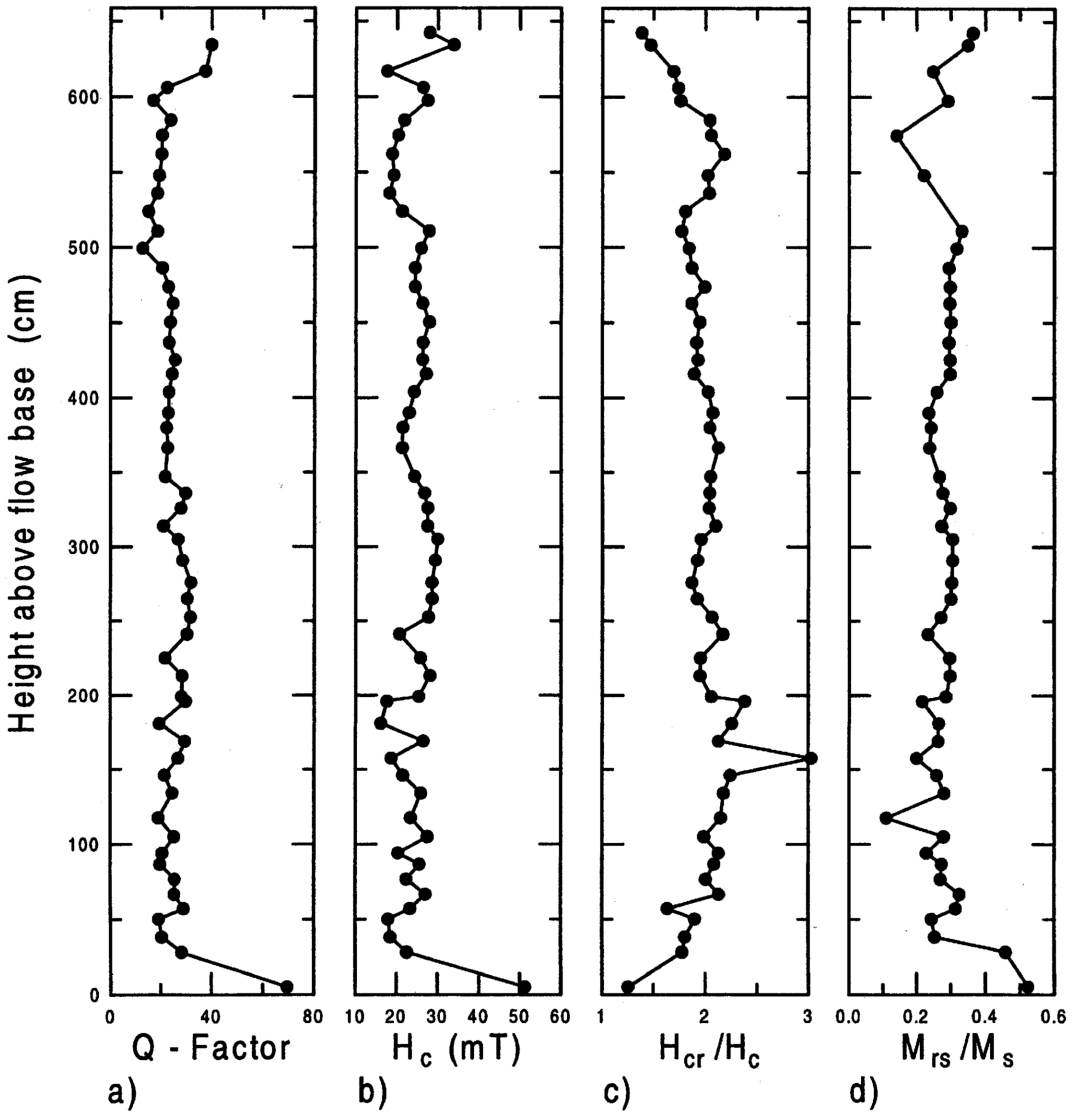

Fig. 7. Variation with height above flow base of coercivity parameters (a) Königsberger Q-factor, (b) coercive force, H_c, (c) ratio of remanent coercive to coercive force, H_{cr}/H_c and (d) reduced saturation magnetisation, M_{rs}/M_s.

The ratio of remanent coercive force to coercive force, H_{cr}/H_c appears to be more sensitive in detecting minor quantities of high coercivity minerals: this ratio varies systematically from base to top, with values around 1.3 at the extremes and maximum values around 2.3 just below 200 cm (Fig. 7(c)). These values are typical for SD and pseudo-SD grains (Day *et al.*, 1977) and the observed trends coincide well with the interpretation of grain size variations discussed above.

Reduced saturation magnetisation M_{rs}/M_s shows similar but less systematic variation with height (Fig. 7(d)). This ratio varies around 0.3 over most of the flow, increasing to approximately 0.5 towards the flow margins. Such values again are typical for pseudo-SD to SD particles.

Figure 8 displays the granulometry parameters in a Day *et al.* (1977) diagram. Most samples have parameters characteristic of pseudo-SD particles, those approaching the SD field representing samples from the margins of the flow where finer grains were observed. As these values correspond to the bulk

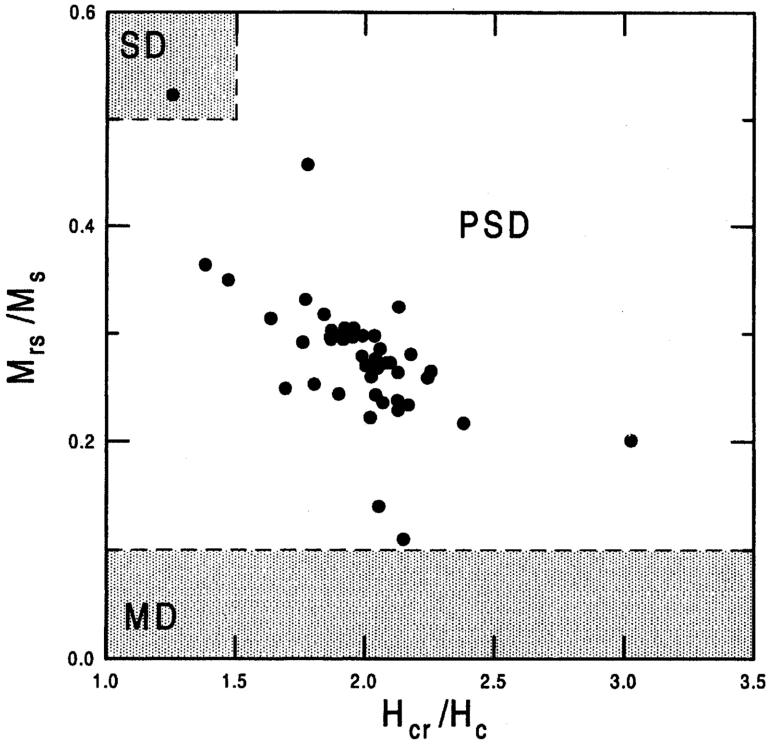

Fig. 8. Day *et al.* (1977) diagram highlighting areas of single domain (SD), pseudo-SD (PSD), and multidomain (MD) behaviour.

minerals, all samples must contain a considerable amount of SD particles. This is an important prerequisite for successful paleointensity determinations (Prévot *et al.*, 1985).

5.3 Summary

In conclusion the magnetic properties are dominated by Ti-poor titanomagnetite (magnetite) in the pseudo-SD grain size range, with grain size decreasing towards the extremes of the flow. This grain size trend is confirmed by visual inspection of polished sections. The discrepancy between the observed grain sizes and those inferred from the magnetic properties is probably due to the highly oxidised nature of the grains. Most show exsolution structures (Fig. 2) which would act to subdivide the apparently MD grains, thus reducing their magnetically effective grain size. The presence of sub-micron grains below the resolution of the microscope may also be having an effect. The grain size and oxidation state of TM throughout the bulk of the flow suggests that it should be suitable for PI experiments. A further observation is the presence of large ilmenite grains which increase in size towards the flow centre and contribute a large paramagnetic signal, especially at low (liquid nitrogen) temperatures.

6. Paleointensities

The temperature steps for the PI experiments were chosen according to the behaviour of pilot samples. Most samples showed maximum unblocking of NRM between 300°C and 570°C and the temperature steps used covered this interval very well.

The component structure of NRM for all samples was analysed using the demagnetisation data provided during the PI experiments. The majority of samples exhibit a univectorial remanence (Fig. 9). For those samples exhibiting secondary components univectorial decay was always observed beyond

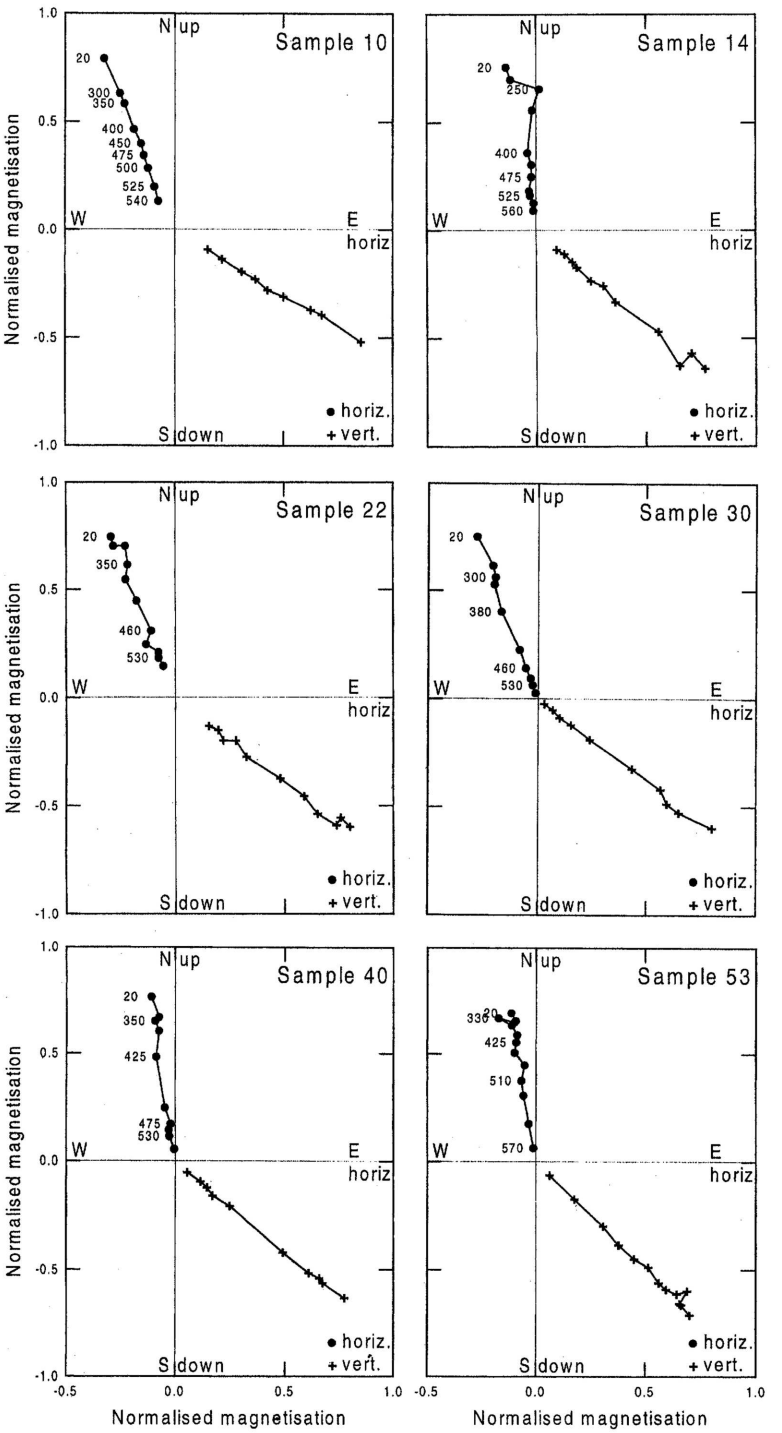

Fig. 9. Component structure of NRM for representative samples. Circles (crosses) denote points in the horizontal (vertical) plane. (Note: the plots are similar to those of Zijderveld, 1967, except that the x and y components are plotted in the horizontal plane and the horizontal, h, and z components are plotted in the vertical plane.)

200–300°C, and a PI may be still recovered between that temperature and 570°C. Characteristic directions were determined by calculating the best-fit line to the remanence vector, excluding those (low temperature) points influenced by secondary components. The resulting directions are shown in Figs. 10(a) and (b). Only 15 samples were taken from cores that were oriented in situ (solid symbols) and these show little directional variation. A further 38 were taken from cores which broke during drilling but nonetheless were able to be given an approximate orientation. They exhibit greater dispersion (open symbols), as might be expected, although their mean direction does not differ significantly from that of the fully oriented samples

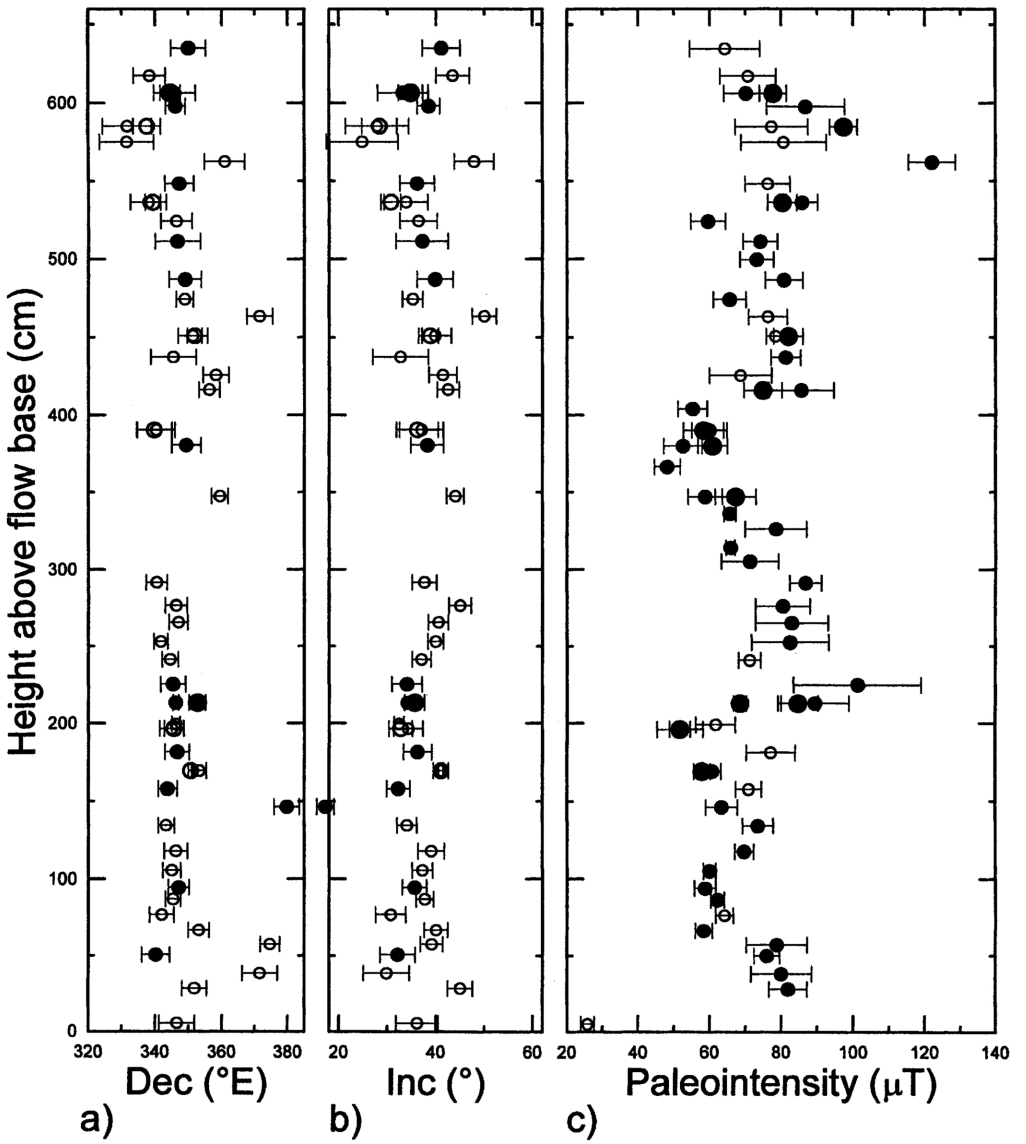

Fig. 10. Variation with height above flow base of (a) declination, Dec, (b) inclination, Inc and (c) paleointensity. For declination and inclination solid (open) symbols denote samples taken from cores oriented in situ (approximately). Error bars are calculated from the maximum angular deviation about the best-fit line to the characteristic remanence vector (Kirschvink, 1980). For paleointensity solid (open) symbols denote accepted (rejected) points. Multiple samples from the same core are differentiated by the larger symbols. Error bars are calculated from the best-fit line on the Arai plot following York (1966).

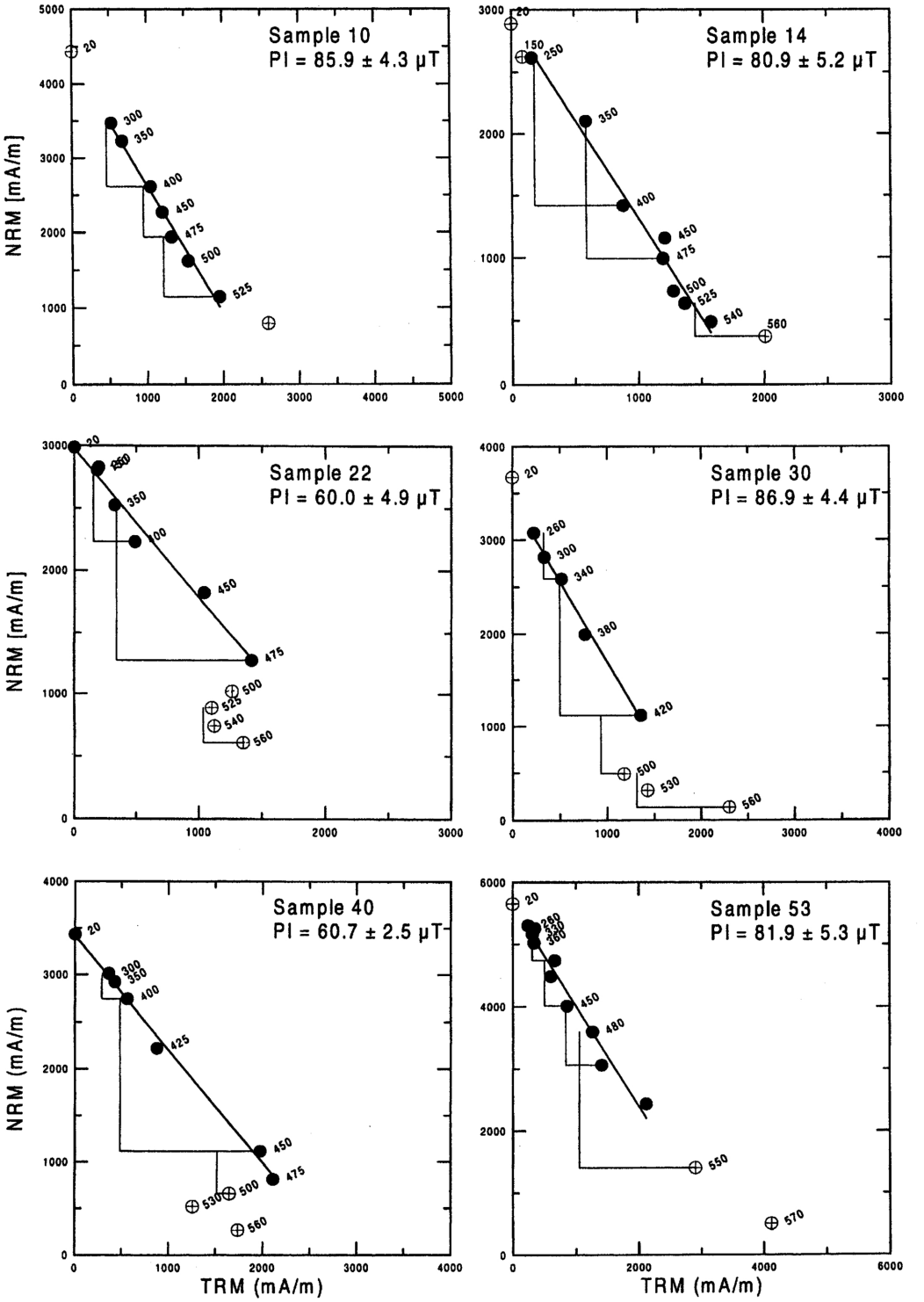

Fig. 11. Arai diagrams for representative samples. Accepted (rejected) points are shown as solid (open) dots. Best-fit lines are based on accepted points only. PI, calculated paleointensity; ±, error of best-fit line (after York, 1966).

(Table 1). The lack of data between 300–400 cm merely reflects a group of unoriented samples.

All PI data derived from the experiments are listed in Table 2 and representative results are shown as Arai plots in Fig. 11. A PI was determined from those samples for which a straight line could be fitted to the data and in this way all samples yielded a PI. Low temperature (<300°C) data was excluded from

Table 1. Mean characteristic directions. Dec, declination; Inc, inclination; α_{95}, 95% cone of confidence about mean direction; k, precision parameter (all after Fisher, 1953); n, number of samples used in the analysis.

Sample set	Dec (°E)	Inc (°)	α_{95} (°)	k	n
Fully oriented	346.7	35.9	1.7	520.6	15
Approximately oriented	347.6	37.8	2.8	71.4	38
All	347.3	37.3	2.0	94.3	53

Table 2. Paleointensity results. pos, height above flow base; N, number of data points used to calculate PI; T range, temperature range over which PI was calculated; g, f, q, the gap, NRM fraction and quality factors, respectively, of Coe *et al.* (1978); nd, not determined; PI, paleointensity result; ±, error of PI result, calculated after York (1966); A/R, result accepted or rejected on the basis of selection criteria (see text). Multiple samples from the same core are denoted by r/r2 and highlighted in bold.

Sample	pos (cm)	N	T range (°C)	g	f	q	PI (μT)	± (μT)	A/R
2	634.5	7	20–475	0.752	0.493	2.4	64.3	9.8	R
3	617.0	8	300–540	0.756	0.746	5.1	70.8	7.8	R
4	606.0	8	300–540	0.848	0.545	5.4	70.2	6.1	A
4.r	606.0	10	20–530	0.875	0.746	13.4	77.8	3.8	A
5	597.5	5	300–475	0.721	0.346	2.0	86.9	10.8	A
6	584.5	4	300–450	0.578	0.245	1.1	77.4	10.2	R
6.r	584.5	9	20–480	0.850	0.429	9.3	97.4	3.8	A
7	574.5	9	250–560	0.868	0.795	4.7	80.7	11.9	R
8	562.0	8	300–540	0.844	0.437	6.9	122.1	6.6	A
9	548.0	3	300–400	0.446	0.210	1.1	76.3	6.3	R
10	536.0	7	300–525	0.817	0.534	8.8	85.9	4.3	A
10.r	536.0	11	20–530	0.865	0.687	11.7	80.4	4.1	A
11	524.0	7	200–500	0.774	0.556	5.3	59.6	4.9	A
12	511.0	7	200–500	0.743	0.591	6.8	74.2	4.8	A
13	499.5	8	200–540	0.824	0.705	9.1	73.2	4.7	A
14	486.5	8	250–540	0.795	0.726	9.1	80.9	5.2	A
15	474.0	7	20–460	0.802	0.701	8.0	65.7	4.6	A
16	463.0	7	20–460	0.793	0.720	8.1	76.4	5.4	R
17	450.5	6	20–460	0.691	0.738	15.4	78.5	2.6	R
17.r	450.5	9	20–480	0.816	0.712	11.7	82.1	4.1	A
18	437.0	7	20–460	0.805	0.712	11.4	81.4	4.1	A
19	425.5	5	20–340	0.728	0.511	2.9	68.7	8.7	R
20	416.0	6	300–480	0.733	0.606	4.2	85.7	9.1	A
20.r	416.0	7	300–480	0.753	0.607	6.4	75.0	5.3	A
21	404.0	6	300–480	0.729	0.526	5.2	55.3	4.1	A
22	390.0	7	20–475	0.768	0.576	5.4	60.0	4.9	A
22.r	390.0	7	300–480	0.768	0.509	4.1	58.4	5.6	A
23	380.0	6	300–480	0.743	0.472	3.4	52.6	5.4	A
23.r	380.0	7	300–480	0.748	0.765	10.2	60.9	4.1	A
24	366.5	6	300–480	0.740	0.470	4.7	48.2	3.6	A
25	347.0	5	300–460	0.675	0.379	3.1	58.8	4.8	A
25.r	347.0	9	20–480	0.810	0.645	6.2	67.3	5.7	A
26	336.0	5	300–480	0.674	0.610	16.9	65.7	1.6	A

the best-fit line where secondary components were observed during NRM demagnetisation. At higher temperatures (generally >500°C) the data points were often seen to deviate from the linear trend and this presumably is due to thermally induced alteration. In some cases this gives rise to an apparent increase in TRM capacity (e.g. samples 10, 14, 53, Fig. 11) and in others a decrease (e.g. samples 22, 30, 40, Fig. 11). Such points were not included in the best-fit line.

Table 2 also lists the statistical parameters of Coe *et al.* (1978). The gap factor (g) in all but 1 sample is greater than 0.5, indicating good data distribution along the best-fit line and for the majority of samples more than half of the remanence is employed in the PI determination. Whilst there is no formal definition of what represents a poor or excellent PI in terms of quality factor (q) the values obtained from this study, ranging from 1.1–24.9, suggests that the PIs are of reasonable to good quality.

7. Discussion

The main objective of this study was to see how PI determinations vary within the flow, irrespective of their quality. For this reason we will first discuss all of the data without any further selection criteria. PI determinations vary within a wide range of 25.8–122.1 μT. The lowest value was obtained from the lowermost sample of the profile (sample 55), which exhibits magnetic properties that are significantly

Table 2. (continued).

Sample	pos (cm)	N	T range (°C)	g	f	q	PI (μT)	± (μT)	A/R
27	326.0	5	250–475	0.662	0.666	4.0	78.6	8.6	A
28	314.0	5	300–480	0.677	0.616	22.9	65.9	1.2	A
29	305.0	5	20–430	0.672	0.713	4.3	71.3	8.0	A
30	291.0	5	260–420	0.677	0.570	7.6	86.9	4.4	A
31	276.0	5	260–420	0.663	0.438	3.1	80.5	7.6	A
32	265.0	5	260–420	0.648	0.433	2.3	83.0	10.1	A
33	252.5	5	260–420	0.669	0.391	2.0	82.5	10.8	A
34	241.0	6	260–500	0.553	0.699	8.9	71.2	3.1	R
35	225.0	5	250–475	0.687	0.583	2.3	101.3	17.8	A
36	213.0	6	260–500	0.647	0.685	4.2	89.4	9.4	A
36.r	213.0	9	20–480	0.810	0.799	24.9	68.5	1.8	A
36.r2	213.0	11	20–540	0.879	0.855	11.4	84.7	5.6	A
37	199.0	5	260–420	0.631	0.427	3.0	61.7	5.5	R
38	196.0	5	260–420	0.579	0.473	2.2	51.8	6.4	A
38.r	196.0	9	20–480	0.803	0.571	8.3	51.7	2.9	A
39	181.0	9	300–560	0.832	0.847	8.1	77.1	6.8	R
40	169.0	7	20–475	0.738	0.770	14.0	60.7	2.5	A
40.r	169.0	8	20–450	0.775	0.777	15.3	57.9	2.3	A
41	157.5	6	300–500	0.695	0.630	8.7	70.9	3.6	R
42	146.0	4	250–475	0.461	0.618	4.2	63.4	4.4	A
43	134.0	7	20–500	0.784	0.737	9.9	73.5	4.3	A
44	117.5	7	20–500	0.775	0.619	13.1	69.7	2.6	A
45	105.0	7	20–475	0.785	0.705	19.5	60.1	1.7	A
46	94.0	7	20–475	0.796	0.655	10.2	58.8	3.0	A
47	86.5	6	20–450	0.775	0.572	14.9	62.3	1.9	A
48	76.5	11	260–550	0.855	0.812	17.8	64.2	2.5	R
49	66.5	10	260–530	0.858	0.659	13.7	58.4	2.4	A
50	57.0	7	260–450	0.806	0.226	1.7	78.8	8.5	A
51	50.0	7	260–450	0.798	0.294	4.9	76.0	3.6	A
52	38.0	7	260–450	0.799	0.258	2.0	80.0	8.5	A
53	28.0	10	260–530	0.848	0.508	6.7	81.9	5.3	A
55	5.0	9	260–510	nd	nd	nd	25.8	1.9	R

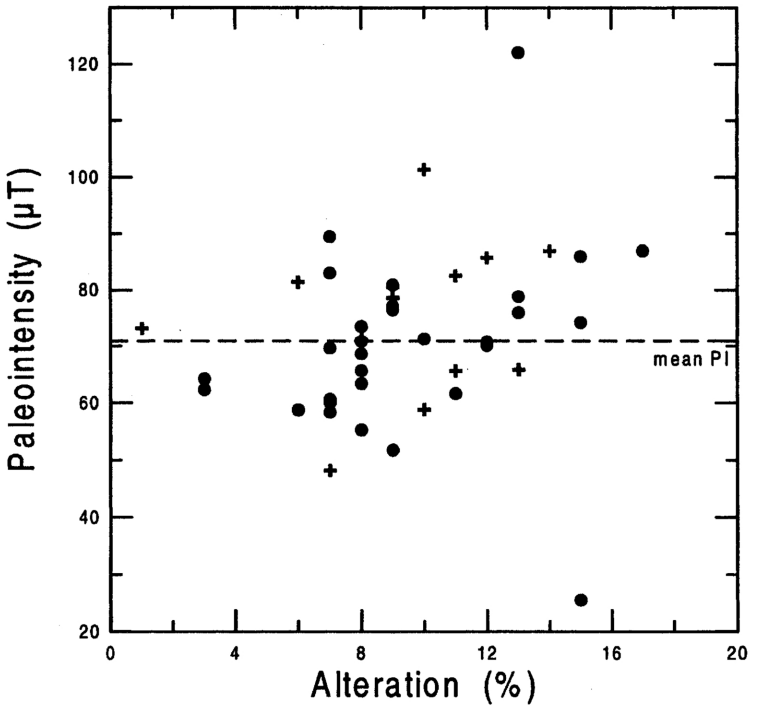

Fig. 12. Paleointensity versus alteration (calculated from the thermomagnetic curves, see text). The flow-mean paleointensity is indicated by the solid line.

different from those of the bulk of the flow. The sample giving the highest PI (sample 8), however, does not show diverging magnetic properties. The rest of the samples have PIs between 48.2 μT and 101.3 μT, which is still a very large range considering that over the last 300 Ma the geomagnetic field apparently has varied in intensity by a similar factor (Tanaka *et al.*, 1995). Surprisingly, when PI is plotted against height (Fig. 10(c)) there appears to be some systematic variation. A large PI swing can be seen between 200–400 cm above the base of the flow with a minimum of 48.2 μT at 370 cm, and a quite broad maximum of 80 μT between 200 cm and 280 cm. The PI extremes are not characterised by abnormally large errors or much smaller values of any quality parameter, and multiple samples from the same core give reproducable results. Therefore the observed variation of PI cannot be explained by experimental errors alone. At this point we should mention that the Xitle flow has cooled down within a time span much shorter than the typical periods of geomagnetic intensity variations: using the estimations from Coe *et al.* (1995) a cooling time of 150 days was obtained. A geomagnetic origin of the observed PI variations is therefore excluded. This is supported by the directional data, which is uniform throughout the flow.

By applying some form of selection criteria we can be more discriminating with the data. In this way we seek to exclude those data which are considered unreliable to see if this affects the observed PI variation. Here we accept a PI if: (a) the best-fit line includes 4 or more points and (b) within the temperature range used to calculate PI pTRM checks pass (i.e. corresponding pTRMs differ by less than 15%). On this basis 51(14) determinations are accepted (rejected), shown as solid (open) symbols in Fig. 10(c). The lowermost value of 25.8 μT (sample 55) is rejected as all pTRM checks fail. It is notable that none of the determinations encompassing the PI swing in the centre of the flow are rejected, nor is the very high determination. Furthermore, excluding the rejected data has no effect on the flow-mean PI. For all data the flow-mean PI has a value of 71.8 μT and a standard deviation of 14.1 μT (n = 65) and these values are 72.6 μT and 14.2 μT (n = 51) when the rejected determinations are excluded.

Comparison of the PI curve in Fig. 10c with the physical and magnetic properties discussed before (Figs. 4–7) shows no apparent correlation. We have used correlation diagrams between each of the physical and magnetic parameters and PI, and there is no evidence that PI depends directly on any of them. The only useful relationship found so far is shown in Fig. 12, where PI is plotted versus the alteration inferred from the thermomagnetic curves. Broadly speaking the higher the alteration, the more PIs diverge from the flow-mean PI. However, even at the highest observed values of this alteration parameter many samples still exhibit PI values close to the flow-mean. This means that despite apparent alteration many samples may still give a "typical" PI.

8. Conclusions

The Xitle lava flow has been sampled along a vertical profile to study the variation of physical and rock magnetic properties and paleointensity. Rock magnetic properties were interpreted in terms of grain size variation and to a minor degree compositional variations. Reliability parameters demonstrated that the obtained PIs were of reasonable to good quality. PI determinations showed significant variation along the profile which was in some part apparently systematic, exhibiting regions of high and low values. This could explain why in different outcrops of the flow different PIs have been obtained, as each outcrop cuts the flow at a certain height, and sampling was typically carried out along a horizontal rather than a vertical line. Samples taken from the same core generally gave reproducable PIs. Application of selection criteria, based on successful pTRM checks, had no affect on the observed variation. Therefore we cannot ascribe the variation solely to experimental errors.

The variation in PI could not be related to any of the measured properties of the flow, physical or magnetic. In this sense these results are different from those of previous studies (Smith, 1967a, b; Ade-Hall *et al.*, 1986b; Rolph, submitted) who recognised associations between PI and other parameters such as grain size/oxidation state. There was a tendency for samples showing relatively more alteration to give PIs which deviated more from the flow-mean PI value, but many altered samples showed PIs close to that mean. It was not possible to differentiate between a "reliable" and an "unreliable" PI on the basis of any of the rock magnetic or visual observations. This leaves the question of what the "correct" value is open. At present all we can do is calculate a flow-mean PI, and for those PIs which satisfied the selection criteria this gave a value of 72.6 μT (standard deviation 14.2 μT) which is consistent with global PI data for this time.

If we are to take the flow-mean PI as a measure of the "true" PI then it is of vital importance that we obtain a sample set that is representative of the flow. What this study has shown is that for the Xitle flow considable variations can be identified vertically. If this is typical for other flows then attention should be paid to sample each flow both horizontally and vertically in order to obtain a more reliable PI.

This work was supported by funds of the UNAM (project IN104994, DGAPA). We would like to thank the Geomagnetism Laboratory at The University of Liverpool and the Palaeomagnetic Laboratory at The University of Utrecht for the use of their Curie balances. Help during the laboratory experiments by José Antonio Gonzalez Rángel is acknowledged. Thanks also to M. Prévot and an anonymous reviewer for their helpful comments.

REFERENCES

Ade-Hall, J. M., M. A. Khan, P. Dagley, and R. L. Wilson, A detailed opaque petrological and magnetic investigation of a single tertiary lava flow from Skye, Scotland—II. Spatial variations of magnetic properties and selected relationships between magnetic and opaque petrological properties, *Geophys. J. R. astr. Soc.*, **16**, 389–399, 1968a.

Ade-Hall, J. M., M. A. Khan, P. Dagley, and R. L. Wilson, A detailed opaque petrological and magnetic investigation of a single tertiary lava flow from Skye, Scotland—III. Investigations into the possibility of obtaining the intensity of the ambient magnetic field (F_{ANC}) at the time of the cooling of the flow, *Geophys. J. R. astr. Soc.*, **16**, 401–415, 1968b.

Audunsson, H., S. Levi, and F. Hodges, Magnetic property zonation in a thick lava flow, *J. Geophys. Res.*, **97**, 4349–4360, 1992.

Coe, R. S., The determination of palaeointensities of the earth's magnetic field with emphasis on mechanisms which could cause non-ideal behavior in Thellier's method, *J. Geomag. Geoelectr.*, **19**, 157–179, 1967.

Coe, R. S., S. C. Grommé, and E. A. Mankinen, Geomagnetic palaeointensities from radiocarbon-dated lava flows on Hawaii and the question of the Pacific non-dipole low, *J. Geophys. Res.*, **83**, 1740–1756, 1978.

Coe, R. S., M. Prévot, and P. Camps, New evidence for extraordinarily rapid change of the geomagnetic field during a reversal, *Nature*, **374**, 687–692, 1995.

Cordova, C. F. de A., A. L. Martin del Pozzo, and J. L. Camacho, Palaeolandforms and volcanic impact on the environment of prehistoric cuicuilco, Southern Mexico City, *J. Archaeol. Sci.*, **21**, 585–596, 1994.

Day, R., M. Fuller, and V. A. Schmidt, Hysteresis properties of titanomagnetites: Grain-size and compositional dependence, *Phys. Earth Planet. Int.*, **13**, 181–190, 1977.

Fisher, R. A., Dispersion on a sphere, *Proc. Roy. Soc. London, Ser. A*, **217**, 295–305, 1953.

Gonzalez-Huesca, I. S., La variacion secular en Mexico central durante los ultimos 30,000 años por medio del estudio magnetico de lavas, Ph.D. Thesis, UNAM, Mexico, 1992 (in Spanish).

Grommé, C. S., T. L. Wright, and D. L. Peck, Magnetic properties and oxidation of iron-titanium oxide minerals in Alae and Makaoputi lava lakes, Hawaii, *J. Geophys. Res.*, **74**, 5277–5293, 1969.

Haggerty, S. E., Oxidation of opaque mineral oxides in basalts, in *Oxide Minerals*, edited by D. Rumble, Mineral. Soc. Am., Short Course Notes, No. 3, 1976.

Herzog, M., H. Bohnel, H. Kohnen, and J. F. W. Negendank, Variation of magnetic properties and oxidation state of titanomagnetites within selected alkali-basalt lava flows of the Eifel-area, Germany, *J. Geophys.*, **62**, 180–192, 1988.

Hunt, C. P., B. M. Moskowitz, and S. K. Banerjee, Magnetic properties of rocks and minerals, rock physics and phase relations, *AGU Reference Shelf*, **3**, 189–204, 1995.

Kirschvink, J. L., The least squares line and plane and the analysis of palaeomagnetic data, *Geophys. J. R. astr. Soc.*, **62**, 699–718, 1980.

Lawley, E. A. and J. M. Ade-Hall, A detailed magnetic and opaque petrological study of a thick palaeogene tholeiite lava flow from Northern Ireland, *Earth. Planet. Sci. Lett.*, **11**, 113–120, 1971.

Libby, W. F., *Radiocarbon Dating*, 2nd edition, University of Chicago Press, Chicago, 1955.

McElhinny, M. W. and W. E. Senanayake, Variations in the geomagnetic dipole 1: the past 50,000 years, *J. Geomag. Geoelectr.*, **34**, 39–51, 1982.

Morales-Contreras, J. J., Determinacion de paleointensidades del campo geomagnetico para el quaternario en la Sierra Chichinautzin, M.Sc. Thesis, UNAM, Mexico, 1995 (in Spanish).

Mullender, T. A. T., A. J. van Velzen, and M. J. Dekkers, Continuous drift correction and separate identification of ferrimagnetic and paramagnetic contributions in thermomagnetic runs, *Geophys. J. Int.*, **114**, 663–672, 1993.

Nagata, T., K. Kobayashi, and E. J. Schwarz, Archaeomagnetic intensity studies of south and central America, *J. Geomag. Geoelectr.*, **17**, 399–405, 1965.

Peterson, N., Notes on the variation of magnetization within basalt lava flows and dykes, *Pageophys.*, **114**, 177–193, 1976.

Prévot, M., E. A. Mankinen, R. S. Coe, and C. S. Grommé, The Steens Mountain (Oregon) geomagnetic polarity transition 2. Field intensity variations and discussion of reversal models, *J. Geophys. Res.*, **90**, 10417–10448, 1985.

Radhakrishnamurty, C., Identification of titanomagnetites by simple magnetic techniques and application to basalt studies, *J. Geol. Soc. India*, **26**, 640–651, 1985.

Rolph, T. C., High field intensity results from recent and historic lavas, *Phys. Earth Planet. Int.*, **70**, 224–230, 1992.

Rolph, T. C., An investigation of the magnetic variation within two recent lava flows, submitted to *Geophys. J. Int.* (submitted).

Senanayake, W. E. and M. W. McElhinny, Hysteresis and susceptibility characteristics of magnetite and titanomagnetite: Interpretation of results from basaltic rocks, *Phys. Earth Planet. Int.*, **26**, 47–55, 1981.

Smith, P. J., On the suitability of igneous rocks for ancient geomagnetic field intensity determination, *Earth. Planet. Sci. Lett.*, **2**, 99–105, 1967a.

Smith, P. J., Ancient geomagnetic field intensities from igneous rocks, *Earth. Planet. Sci. Lett.*, **2**, 329–330, 1967b.

Sternberg, R. S., Archaeomagnetic palaeointensity in the American southwest during the last 2000 years, *Phys. Earth Planet. Int.*, **56**, 1–17, 1989.

Tanaka, H., M. Kono, and H. Uchimura, Some global features of palaeointensity in geological time, *Geophys. J. Int.*, **120**, 97–102, 1995.

Watkins, N. D. and S. E. Haggerty, Some magnetic properties and the possible petrogenetic significance of oxidized zones in an Icelandic olivine basalt, *Nature*, **206**, 797–800, 1965.

Wilson, R. L., S. E. Haggerty, and N. D. Watkins, Variation of palaeomagnetic and other parameters in a vertical traverse of a single Icelandic lava, *Geophys. J. R. astr. Soc.*, **16**, 79–96, 1968.

York, D., Least squares fitting of a straight line, *Can. J. Phys.*, **44**, 1079–1086, 1966.

Zijderveld, J. D. A., A.C. demagnetization of rocks: Analysis of results, in *Methods in Palaeomagnetism*, edited by D. W. Collinson, K. M. Creer, and S. K. Runcorn, pp. 254–286, Elsevier, Amsterdam, 1967.